

8. Клето Г. И. Наноразмерные сегнетоэлектрические пленки для интегральных запоминающих элементов / Г. И. Клето, Я. В. Мартынюк, А. И. Савчук и др. // Наносистемы, наноматериалы, нанотехнологии, Nanosystems, Nanomaterials, Nanotechnologies. – 2009. – Т.7, №1.– С. 65-71.
9. Sidorkin A. S. Parameters of Domain Boundaries in Thin PbTiO<sub>3</sub> Films / A. S. Sidorkin, L. P. Nesterenko, A. L. Smirnov etc. // Ferroelectrics. – 2007. – V. 359, N 1-6.
10. Zhou X. Y. Microstructure and enhanced in-plane ferroelectricity of Ba<sub>0.7</sub>Sr<sub>0.3</sub>TiO<sub>3</sub> thin films grown on MgAl<sub>2</sub>O<sub>4</sub> (001) single-crystal substrate / X. Y. Zhou, T. H. Heindl, G. K. Pang etc. // Appl.Phys.Lett. – 2006. – V. 89. – P. 232906-1–232906-3.
11. Wang S. Y. Raman spectroscopy studies of Ce-doping effects on Ba<sub>0.5</sub>Sr<sub>0.5</sub>TiO<sub>3</sub> thin films [Text] / S. Y. Wang, B. L. Cheng, C. Wang etc. // J.Appl.Phys. – 2006. – V. 99. – P. 013504-1-013504-6.

*Надійшла до редакції  
22 липня 2015 року*

© Воронов С. О., Богорош О. Т., Муравов С. О., Гордійко Н. О., 2015

УДК 621.389; 621.3.01

## NUMERICAL CALCULATION OF TEMPERATURE DISTRIBUTION IN CRUCIBLE OF INDUCTION EVAPORATOR WITH MAGNETIC FIELD CONCENTRATOR

*Tsibulskiy L. Yu.*

*National Technical University of Ukraine «Kyiv polytechnic institute», Kyiv, Ukraine*

*E-mail: [senti-ki@ukr.net](mailto:senti-ki@ukr.net)*

*The article describes the methodology and results of hierarchical modeling of the induction evaporator with electromagnetic field concentration, which takes into account the related heterogeneous processes and allows to numerically calculate the electromagnetic field in the vicinity of the evaporator as well as current and temperature distributions in the loaded crucible. The model development work allows to make the conclusion that the method of finite elements is most suitable for calculation of electromagnetic and temperature fields. The given model may be employed for modeling vapor flow ejection from the crucible to substrates and electrical discharges in the evaporator.*

**Keywords:** *HF heating simulation, induction evaporator, crucible, volatile substance, numerical method*

### **Introduction**

The important part of microelectronic fabrication is deposition of thin layers or films from solid materials onto substrates. The usual deposition method is a vacuum evaporation of source materials. This method may be realized with different heaters including induction one [1]. In order to match high output impedance of RF generator with low impedance of the inductor-heater, a step-down RF transformer is commonly employed. The aim of the given work is numerical simulation of the induction evaporator with step-down RF transformer containing a magnetic field concentrator and study of its characteristics. Introducing the concentrator into the evaporator allows solving several practical problems; one of them is providing stable arcless operation of the evaporator, the other is increasing effectiveness of power transfer.

Induction evaporators are able to continuously operate in vacuum or in gas media up to atmospheric pressure. Also they provide evaporation with generation of charged particles or without this generation. The former gives possibility to manage ion bombardment of the deposited film with own ions that is to introduce additional energy into film microstructure forming and enhance the film properties [2]. Moreover, no gas ions are needed and, hence, introducing gas impurities into the film may be excluded. The latter ensures deposition with very low impact energy (below 0.1 eV) that is very useful for temperature-sensitive materials of either substrate or deposited film. At last, the induction method allows evaporating various materials for thin film deposition and also to obtain substance in nanoparticulate form, including fullerenes and carbon nanotubes for nanodevices and nanotechnology, in general.

Despite prospects of induction evaporation, its use is underdeveloped due to lack of methods for analysis and optimization of evaporators design. One of the problems is eliminating electrical discharges between inductor windings being in vapor medium; this problem is not solved. High voltage between the windings (hundreds volts) provokes the electrical discharges, so this should be decrease at the same intensity of induction evaporation. We propose to introduce an additional step-down transformer between the heating inductor and the crucible. This transformer, in fact, is well-known magnetic field concentrator [1, 3].

The goal of research is producing computer models and study the processes occurring in induction evaporator with the magnetic field concentrator, as well as determination of the geometric dimensions effect upon characteristics of evaporator.

### **Induction evaporator with magnetic field concentrator**

Fig. 1 depicts the simplified design of such induction evaporator with the magnetic field concentrator and its graphical model for numerical calculation.

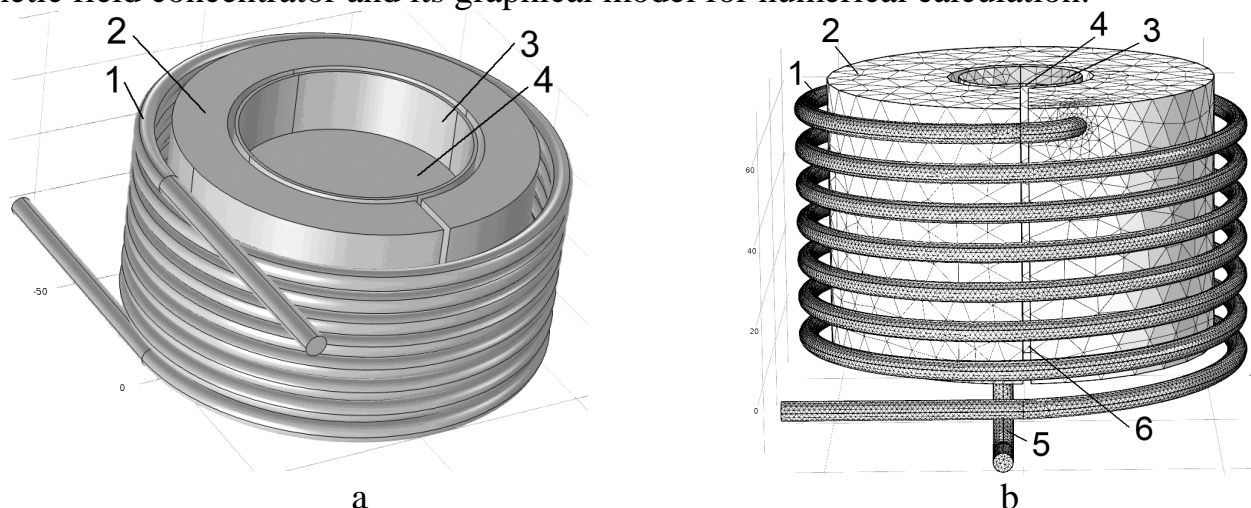


Fig. 1. Design of induction evaporator with magnetic field concentrator: 1 – primary inductor (copper tube), 2– concentrator (copper hollow body), 3 – crucible, 4 – vaporized loading (melted metal), 5 – electrical terminal (copper tube, connecting with internal cavity of the concentrator), 6 – radial gap (cutting) in the concentrator

Concentrator 2 is a conductive body with radial gap (cutting) 6. Its cylindrical external and internal surfaces are, in fact, two turns connected in series. This body concentrates the magnetic field flow of big primary inductor 1 within the smaller internal turn. In Fig. 1a, primary inductor 1 and concentrator 2 are electrically isolated each from other; in Fig. 1b, they are connected in series. Accordingly, RF generator is connected either directly to the inductor (Fig. 1a) or to the lower inductor winding and to tube 5 (Fig. 1b). Crucible 3 is electrically isolated from concentrator 2 in the both cases. Inductor 1 and concentrator 2 are cooled by water. Vaporized metal 4 (Ag, Al, Au, Cu, In, Sn, *etc.*) is loaded into the crucible. The crucible may be from conducting (*e.g.* Mo) or non-conducting materials (*e.g.* BN). Fig. 1b depicts the finite element mesh for calculation.

### Structure of the model and calculations

For the analysis of the processes occurring in the evaporator one creates a physical model taking into account the combination of those processes. Herein, during simulation the calculated results for one process parameter are used for calculation of parameters of other processes. The hierarchical structure of the physical model is presented in Figure 2. In this structure, lines between blocks indicate data transfer, directions of which are top-down and down-top.

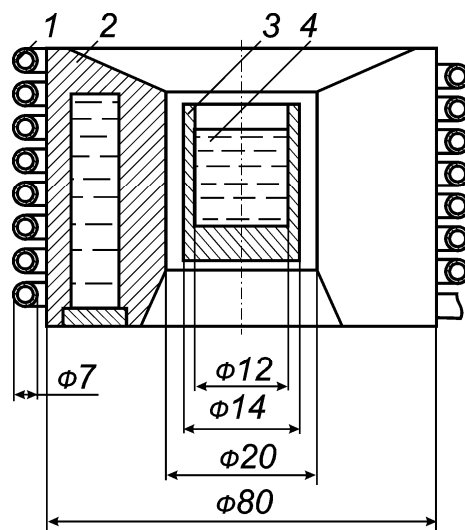
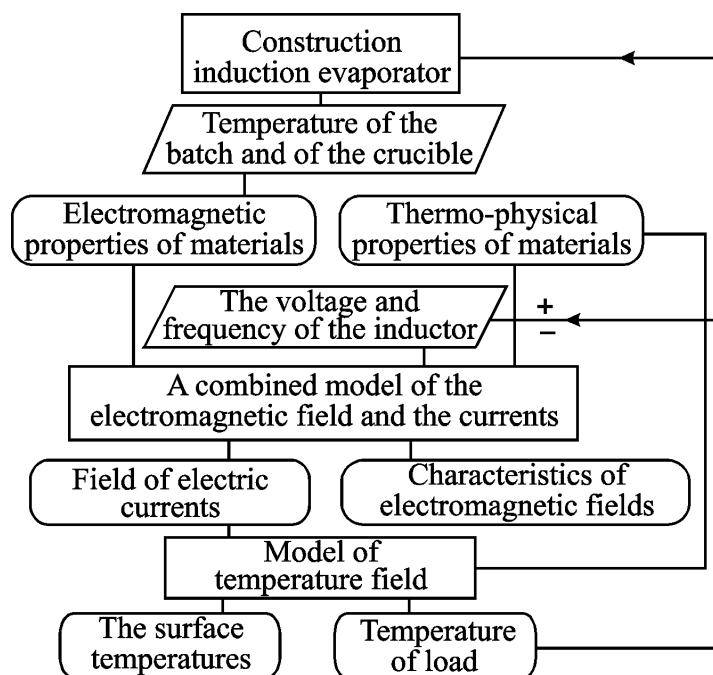


Fig.2. Structure of physical model of the induction evaporator

Fig. 3. Construction of the induction evaporator with the concentrator: 1 – inductor 2 – concentrator 3 – crucible 4 – vaporized loading (the dimensions are in millimeters)

The latter is indicated by arrows and depicts the feedback to correct solutions after the following iteration due to evaluation of calculation results for the previous iteration.

The initial data for the calculation are:

- 1) induction heater design and the number of windings; dimensions of all elements;
- 2) required operating temperature of crucible and loading (evaporated source material)  $T$ ;
- 3) physical properties of element materials at operating temperature (density, electrical conductivity, magnetic permeability and its dependence on the magnetic field  $H$  in the case of magnetic heated loading, specific heat, thermal conductivity, radiation coefficient from surface of the crucible and loading;
- 4) initial voltage and frequency of RF power supply of the primary inductor.

To determine the temperature distribution (temperature field) we use induction-heating models associated with numerical solutions of Maxwell equations for electromagnetic field (EMF) and Fourier equation for temperature field [4]. As a result, the temperature field in a selected area at given voltage across the inductor for dynamic or stationary process is determined.

One needs to solve two combined different tasks:

1. The direct task for definition the EM field according to some inductor current and currents in elements of the evaporator induced by this field;
2. The inverse task for defining currents in the crucible and with loading needed to reach the predetermined temperature of heating.

We use the following algorithm for solving our problem. Firstly, determine distribution of EMF in the evaporator space and currents in the conductive elements (taking into account ohmic losses in their materials) at the predetermined frequency and voltage of inductor power supply. Then distribution of heat sources in the heated elements (crucible, load) is determined. Then task of finding temperature fields in the heated element is solved. After this we determine temperature of the evaporating surface of the source material. The calculation is repeated again until the voltage on the inductor is determined according to the predetermined temperature value.

The proposed algorithm allows to calculate EMF and temperature fields, electric voltage and conditions on the evaporating surface in the crucible and, ultimately, to analyze parameters of the vapor flow toward the substrate.

### **Model of electromagnetic field**

The combined mathematical model of EMF and currents is based on partial differential equations for complex amplitude of vector magnetic potential  $\mathbf{A}$ . Magnetic induction vector  $\mathbf{B}$  lies in plane  $zOr$  ( $z$  is the axial coordinate,  $r$  is the radius). The vector density of electric current  $\mathbf{j}$  and the vector magnetic potential  $\mathbf{A}$  are orthogonal to  $\mathbf{B}$ . Only the azimuthal components  $j_\theta$  and  $A_\theta$  are non-zero and will be marked as  $j$  and  $A$ . For the axisymmetric model we obtain

$$\frac{\partial}{\partial r} \left( \frac{1}{r\mu_z} \frac{\partial(rA)}{\partial r} \right) + \frac{\partial}{\partial z} \left( \frac{1}{\mu_r} \frac{\partial A}{\partial z} \right) - i\omega \cdot \gamma \cdot A = -j_{\text{outs}},$$

where electrical conductivity  $\gamma$  and magnetic permeability tensor elements  $\mu_z$  and  $\mu_r$  are constants within each element in the model. The displacement current is neglected –  $rot \mathbf{H}=0$ . Materials of the inductor, crucible and loading we consider as isotropic, while the electrical conductivity is independent from direction and intensity of the electric field and connected with them by Ohm's law.

At boundaries of computational domain, value of zero vector magnetic potential  $\mathbf{A}$  is given. Dirichlet condition for the boundaries of medium (elements) is given as a function of coordinates:  $r\mathbf{A}_0=a+bzr+cr^2/2$ , where  $a$ ,  $b$  and  $c$  are constants for each surface and may vary from one surface to another.

Uniform external field is given by non-zero normal component of magnetic induction on each smooth section of boundary between media. On the axis of symmetry, the model has been set homogeneous Dirichlet boundary condition: the value of normal component is zero ( $B_r = 0$ ).

If  $\alpha$  - surface angle to axis  $z$ , then normal component of induction  $B_x = c \cdot \sin\alpha + b \cdot \cos\alpha$  constant value on different surfaces is chosen according to the Dirichlet conditions, under the condition of  $A_0$  continuity at interface (mating surfaces).

The homogeneous Neumann boundary conditions is given on the surfaces of magnetic asymmetry: at external borders  $H_t = \sigma$ , at internal border  $H_t^+ - H_t^- = \sigma$ , where  $H_t$  is the tangential component of magnetic field. The indices "+" and "-" indicate value to the left or right surfaces, relatively.  $\sigma$  is the linear density of surface current, which is determined by calculations.

In calculations, following values are defined:

1. Magnitude and distribution of currents in crucible and loading;
2. Distribution of magnetic and electric fields in the evaporator that can be used in the model of vapor material discharge;
3. Ohmic losses that are used as heat source during calculation of the temperature field in the crucible and loading.

Fig. 3 depicts design of the evaporator with the concentrator, which was used in the simulation. The concentrator 2 is a short cylinder with a cutting in one side along the radius. The current in the outer cylindrical surface of the concentrator is driven by alternative inductor current and is closed at the inner cylindrical surface along the surfaces of the radial cutting 6 (Fig. 1b). Inside the concentrator, the crucible, made from refractory material 3 (molybdenum, tantalum, boron nitride, etc.) with loading substance 4 is disposed.

### Calculation of current and magnetic field distribution

Fig. 4 shows current distributions along the radial cutting of the evaporator in the picture plane of Fig. 3 at frequency of 440 kHz for the case when the evaporator contains inductor non-connected with concentrator (see Fig. 1a). Theoretically, all the curves should provide exponents with initial maximal amplitude on surface and falling within metal. Deviation from the exponential law is connected with insufficient accuracy of calculation (small number of nodes), due to limited computer processing

power. But it is not important for our calculations. The sum of current values (1), in the wall of crucible 3, and (2), under the inner surface of concentrator 2, are theoretically equal to current (3) under the outer surface of concentrator 2. These currents are equal to the area of the shaded regions in Fig. 4. Calculations confirm this fact.

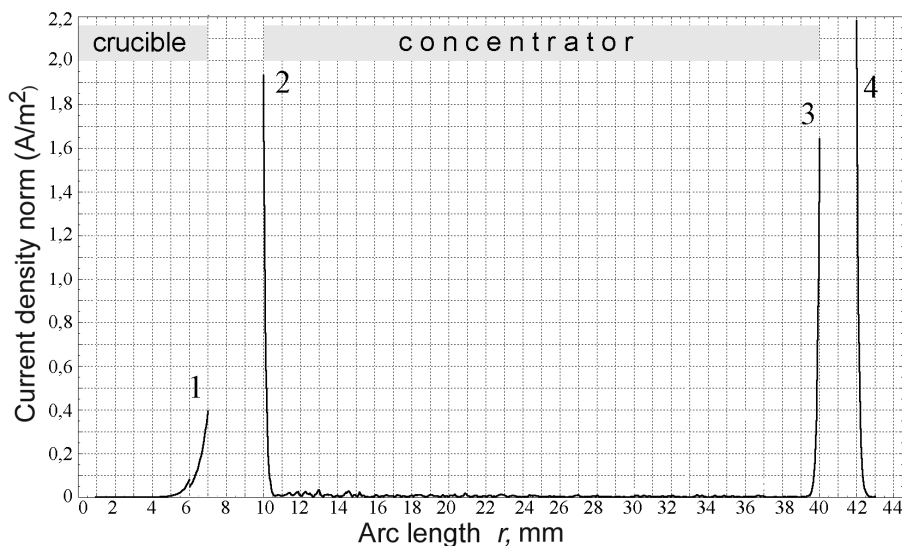


Fig. 4. Calculated current distributions in the evaporator: 1 – in crucible wall, 2 – under the inner surface of concentrator, 3 – under the outer surface of the concentrator, 4 – in inductor. Dashed lines for: a is the crucible surface, b is the inner concentrator surface, c is the outer concentrator surface, d is the evaporator axis

The example of the calculated magnetic field distribution in the symmetry plane is presented in Fig. 5 as a tone map. The map allows visual assessment of design parameters impact on the field distribution and the localization of the greatest strength. Family of lines in Fig. 5 represents lines of equal magnetic flux.

Fig. 6 shows magnetic field variation graphs along the radius. For clarity, counting takes part from the inner wall of concentrator to its axis. Z values in the graphs are expressed in mm and measured from the inner wall top.

### Temperature field determining

Temperature field model of the crucible-loading system is based on numerical calculations by finite difference method for nonlinear heating equation in cylindrical coordinates [5].

All thermal properties of materials: thermal conductivity  $\lambda(T)$ , specific heat capacity  $q(T)$ , specific heat  $c(T)$  and density  $\rho$  are chosen from literature data correspondingly to loading evaporation temperature.

For the stationary task  $c(T)\frac{\partial T}{\partial t} = 0$ . Then the heating equation becomes:

$$\frac{1}{r} \frac{\partial}{\partial r} \left( \lambda(T) \rho \frac{\partial T}{\partial r} \right) + \frac{\partial}{\partial z} \left( \lambda(T) \frac{\partial T}{\partial z} \right) = -q(T).$$

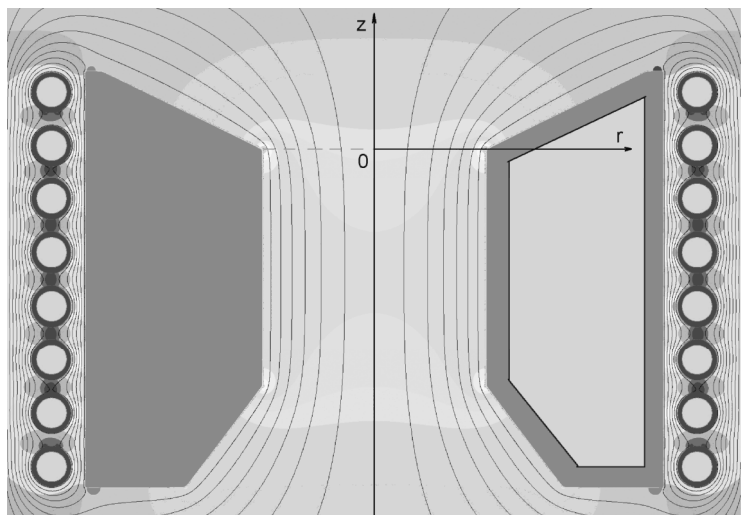


Fig. 5. Tone magnetic field map in the symmetry plane of the evaporator with magnetic field lines (the inner diameter equals 30 mm)

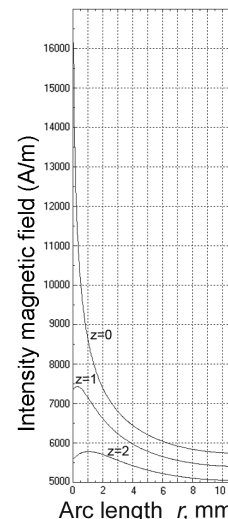


Fig. 6. Dependence of magnetic field intensity along the radius from the inner wall toward the axis of concentrator having inner diameter 22 mm

Heat exchange processes for using metallic or dielectric crucible are identical. If crucible is electrically conductive, the loading is mainly heated by heat flow from the crucible wall. When crucible is electrically insulated, heat sources arise directly in surface layers of the loading.

The calculations are based on finite element method [4] with a grid consisting of 250000 units. Properties of materials used in the model were determined from reference literature for pure chemicals. Thermal properties of the crucibles were taken from [6-8].

The distribution of heat sources repeats the current distribution in the crucible and loading (see. Fig.3) and is determined by Joule law.

During calculation the inductor temperature was taken 50 C that corresponds to the temperature of cooling water. The evaporator was placed in vacuum with no convective heat transfer. The surrounding walls was 300 K.

The boundary conditions (of the second kind) take into account the radiative heat fluxes from the outer surface of the crucible and the evaporating surface. Herein, radiative heat fluxes depend on the surface temperature  $T$ :

$$q_{\text{изл}} = k \cdot \alpha (T^4 - T_0^4),$$

where  $k = 5,6704 \cdot 10^{-8} \text{ Wt/(m}^2 \cdot \text{grad}^4)$  – Stefan-Boltzmann constant,  $\alpha$  – surface absorption coefficient, and  $T_0$  – the temperature of the environment. The parameters  $\alpha$  and  $T_0$  may be different on different surfaces of the evaporator.

The surface of the crucible is taken as polished. The emissivity data for pure materials is taken from literature.

The heat loss from the loading is considered only as the loss on the evaporation from the open surface:  $q_{исп} = W \cdot L$ , where  $W$  is the rate of evaporation of the loading substance in  $\text{kg}/(\text{m}^2 \cdot \text{s})$ ;  $L$  is the latent heat of vaporization,  $\text{J}/\text{kg}$ . The data on  $L$  were taken from [9, 10].

### Calculating of temperature field in crucible with loading

Temperature fields maps in the molybdenum crucible with copper loading (a) and  $\text{TiB}_2 + \text{TiC}$  crucible with aluminum loading (b) at frequency of inductor current  $f = 440 \text{ kHz}$  are shown in Fig. 7. Isotherms are depicted with steps of  $0.5 \text{ K}$ .

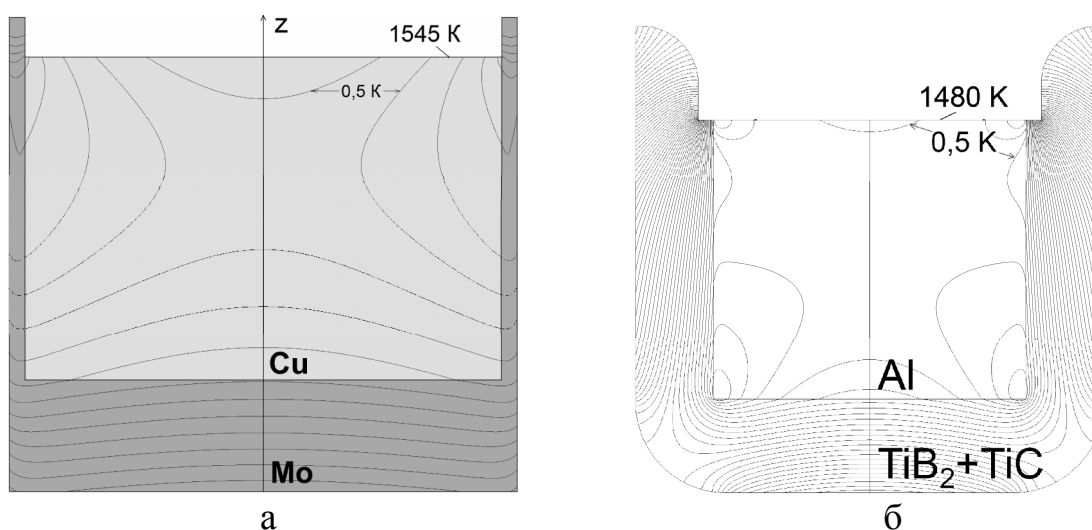


Fig. 7. Maps of temperature fields in loadings and crucibles: a) copper in the molybdenum crucible, and b) aluminum in the  $\text{TiB}_2 + \text{TiC}$  crucible

Isotherms enable conclusion that the temperature gradient in copper loading is  $1.5 \text{ K}$  and  $2.2 \text{ K}$  in aluminum.

The maps were obtained without magnetic hydrodynamic convection and mixing, which are bigger at the free surface of the molten loading than at the crucible bottom. The recoil force of evaporating molecules (uniformly distributed along the loading surface) was not taken into account. It can be assumed that the actual temperature drop along the evaporating surface of loading is less than  $1 \text{ K}$ .

Fig. 8 shows the calculated temperature distribution plots along the copper loading surface for number of inductor current frequency. The calculations were made for the mean evaporating surface temperature  $1545 \text{ K}$ .

The calculation show that the temperature difference on the loading surface weakly depends on the inductor current ( $3 \text{ K}$  for aluminum and  $2 \text{ K}$  for copper). Thus, it may be accepted the term of isothermal evaporation surface.

### Conclusions

The hierarchical modeling of the induction evaporators, which takes into account the related heterogeneous processes and gives the data on electromagnetic field in the vicinity of the evaporator as well as current and temperature distributions in the

loaded crucible, is carried out. The model development work allows to make the conclusion that the method of finite elements is most suitable for calculation of electromagnetic and temperature fields.

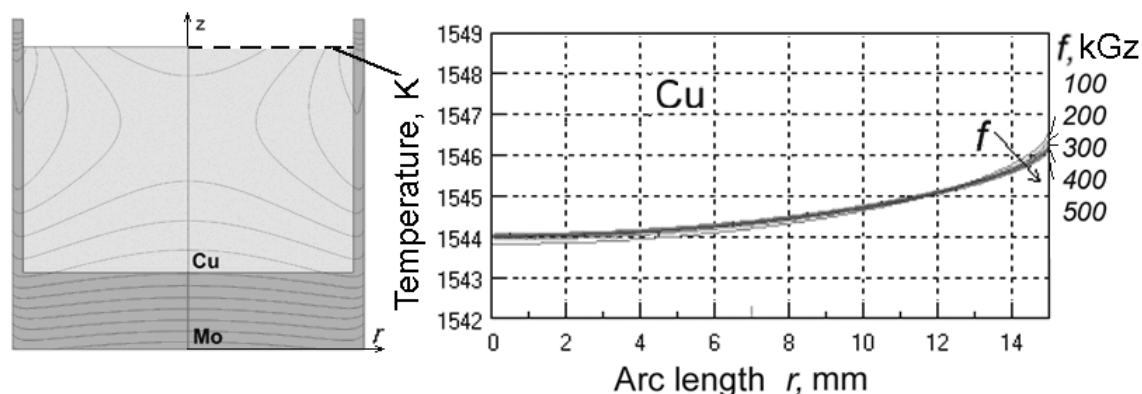


Fig. 8. Temperature distribution on surface of Cu load from middle to crucible wall at different frequencies of inductor current

The calculation results show that the evaporating metal surface may be considered as isothermal (with error less than 0.01 %).

The given model may be employed for modeling vapor flow ejection from the crucible and electrical discharges in the evaporator in the future.

#### References

1. Kuzmichev A. Evaporators with Induction Heating and Their Applications. Chapter 13 (P. 269-302) in book «Advances in Induction and Microwave Heating of Mineral and Organic Materials». / A. Kuzmichev, L. Tsybul'skiy // Ed. S. Grundas. – ISBN: 978-953-307-522-8. – Publisher: InTech, 2011. – 752 p.
2. Kuzmichev A.I. Thermoionic unit with inductive evaporator / A. I. Kuzmichev, L.Yu. Tsybul'skii. // Instruments and Experimental Techniques. – 1992. – V. 35, – No. 2. – P. 379-380.
3. Слухоцкий А. Е. Индукторы для индукционного нагрева / А.Е. Слухоцкий, С.Е. Рыскин // – Л. : Энергия, 1974. – 264 с.
4. Зенкевич О. Конечные элементы и аппроксимация / О. Зенкевич, К. Морган. – М.: Мир, 1986. – 318 с.
5. Исаченко В. П. Теплопередача: учебник для вузов. – 3-е изд. / В. П. Исаченко, В. А. Осипова, А. С. Сукомел. – М.: Энергия, 1975. – 488 с.
6. Зиновьев В.Е. Теплофизические свойства металлов при высокой температуре: справ.изд. / В.Е. Зиновьев. – М.: Metallurgy, 1989. – 384 с.
7. Грановский В. Л. Электрический ток в газе. Т.1. / В. Л. Грановский. – М.-Л.: Гос. из-во техн.-теорет. лит, 1952. – 432 с.
8. Термодинамические свойства индивидуальных веществ: справ. изд. / под ред. В. П. Глушко. – М.: Наука, 1981. – 400 с.
9. Дешман С. Научные основы вакуумной техники. – М.: Мир, 1964. – 715 с.
10. Самсонов Г. В. Свойства элементов. В 2 ч. Ч1. Физические свойства: справочник. – М.: Metallurgy, 1976. – 600 с.

Надійшла до редакції  
28 серпня 2015 року

© Tsibul'skiy L. Yu., 2015